JCI The Journal of Clinical Investigation

RETRACTED

View retraction

Amendment history:
- Retraction (December 2012)

Connexin 43 acts as a cytoprotective mediator of signal transduction by stimulating mitochondrial K_{ATP} channels in mouse cardiomyocytes

Dennis Rottlaender, … , Gerd Heusch, Uta C. Hoppe

J Clin Invest. 2010;120(5):1441-1453. https://doi.org/10.1172/JCI40927.

Research Article Cardiology

Potassium (K^+) channels in the inner mitochondrial membrane influence cell function and survival. Increasing evidence indicates that multiple signaling pathways and pharmacological actions converge on mitochondrial ATP-sensitive K^+ (mitoK_{ATP}) channels and PKC to confer cytoprotection against necrotic and apoptotic cell injury. However, the molecular structure of mitoK_{ATP} channels remains unresolved, and the mitochondrial phosphoprotein(s) that mediate cytoprotection by PKC remain to be determined. As mice deficient in the main sarcolemmal gap junction protein connexin 43 (Cx43) lack this cytoprotection, we set out to investigate a possible link among mitochondrial Cx43, mitoK_{ATP} channel function, and PKC activation. By patch-clamping the inner membrane of subsarcolemmal murine cardiac mitochondria, we found that genetic Cx43 deficiency, pharmacological connexin inhibition by carbenoxolone, and Cx43 blockade by the mimetic peptide ^{43}GAP27 each substantially reduced diazoxide-mediated stimulation of mitoK_{ATP} channels. Suppression of mitochondrial Cx43 inhibited mitoK_{ATP} channel activation by PKC. MitoK_{ATP} channels of interfibrillar mitochondria, which do not contain any detectable Cx43, were insensitive to both PKC activation and diazoxide, further demonstrating the role of Cx43 in mitoK_{ATP} channel stimulation and the compartmentation of mitochondria in cell signaling. Our results define a role for mitochondrial Cx43 in […]

Connexin 43 acts as a cytoprotective mediator of signal transduction by stimulating mitochondrial K_{ATP} channels in mouse cardiomyocytes

Dennis Rottlaender,[1] Kerstin Boengler,[2] Martin Wolny,[1] Guido Michels,[1] Jeannette Endres-Becker,[1] Lukas J. Motloch,[1] Astrid Schwaiger,[1] Astrid Buechert,[2] Rainer Schulz,[2] Gerd Heusch,[2] and Uta C. Hoppe[1,3]

[1]Department of Internal Medicine III, University of Cologne, Cologne, Germany. [2]Institute for Pathophysiology, University of Essen, Essen, Germany. [3]Center for Molecular Medicine, University of Cologne (CMMC), Cologne, Germany.

Potassium (K^+) channels in the inner mitochondrial membrane influence cell function and survival. Increasing evidence indicates that multiple signaling pathways and pharmacological actions converge on mitochondrial ATP-sensitive K^+ (mitoK_{ATP}) channels and PKC to confer cytoprotection against necrotic and apoptotic cell injury. However, the molecular structure of mitoK_{ATP} channels remains unresolved, and the mitochondrial phosphoprotein(s) that mediate cytoprotection by PKC remain to be determined. As mice deficient in the main sarcolemmal gap junction protein connexin 43 (Cx43) lack this cytoprotection, we set out to investigate a possible link among mitochondrial Cx43, mitoK_{ATP} channel function, and PKC activation. By patch-clamping the inner membrane of subsarcolemmal murine cardiac mitochondria, we found that genetic Cx43 deficiency, pharmacological connexin inhibition by carbenoxolone, and Cx43 blockade by the mimetic peptide ^{43}GAP27 each substantially reduced diazoxide-mediated stimulation of mitoK_{ATP} channels. Suppression of mitochondrial Cx43 inhibited mitoK_{ATP} channel activation by PKC. MitoK_{ATP} channels of interfibrillar mitochondria, which do not contain any detectable Cx43, were insensitive to both PKC activation and diazoxide, further demonstrating the role of Cx43 in mitoK_{ATP} channel stimulation and the compartmentation of mitochondria in cell signaling. Our results define a role for mitochondrial Cx43 in protecting cardiac cells from death and provide a link between cytoprotective stimuli and mitoK_{ATP} channel opening, making Cx43 an attractive therapeutic target for protection against cell injury.

Introduction

Ischemic injury can result in cell death and irreversible loss of function in a variety of biological systems (1, 2). Understanding of the intracellular signaling mechanisms by which cells protect themselves against ischemia-induced damage bears great clinical significance with respect to the treatment and prevention of tissue injury (3). A powerful cytoprotective adaptation can be produced by brief episodes of ischemia followed by reperfusion before sustained ischemia or by pharmacological agents such as diazoxide mimicking these preconditioning effects (1, 2). Ischemic preconditioning (IP) leads to release of hormones or agonists that bind to G protein–coupled receptors and activate signaling pathways (1, 4). Mitochondria are essential targets and effectors in these cytoprotective cascades (1, 5). Particularly, it has been suggested that opening of the mitochondrial adenosine triphosphate–sensitive K^+ (mitoK_{ATP}) channel and activation of cytosolic and mitochondrial protein kinase C (PKCε) play a critical role in protection against ischemic cell injury (1, 6, 7). However, the molecular structure of mitoK_{ATP} channels remains unresolved, and no mitochondrial phosphoprotein has yet been identified that may mediate cytoprotection by these kinases (6, 8).

Conflict of interest: The authors have declared that no conflict of interest exists.
Citation for this article: *J Clin Invest.* 2010;120(5):1441–1453. doi:10.1172/JCI40927.

Cytoprotection by both pharmacological and IP is abolished in transgenic animals with connexin 43 deficiency (9–11). Connexin 43 (Cx43), the main gap junction protein, is predominantly localized in the sarcolemma but is also found in the inner mitochondrial membrane (Figure 1) (10, 12). To determine how mitochondrial Cx43 might be involved in the preconditioning pathway, we used direct single-channel patch-clamp recordings of cardiac mitoplasts to identify a possible link among mitoK_{ATP} channel function, mitochondrial Cx43, and PKC activation.

Results

By patch-clamping the inner membrane of subsarcolemmal mitochondria (mitoplasts) prepared from isolated cardiomyocytes, we verified the existence of mitochondrial K_{ATP} channels in wild-type mice. In K^+ solution (150 mM KCl), voltage-dependent single-channel currents with a unitary conductance of 13.7 ± 0.3 pS, an amplitude of –0.83 ± 0.05 pA, and an open probability of 0.29% ± 0.08% (Po,total; at –60 mV, n = 22) were obtained (Figure 2, A and B, Figure 3, B and C, and Table 1). These currents could be activated by the mitoK_{ATP} channel opener diazoxide (100 μM), which significantly increased the open probability (Po,total, 4.30% ± 0.40%, n = 16, P < 0.05) and mean open time without affecting single-channel amplitude and conductance (Figure 2A, Figure 3, B, C, and E, and Table 1). MitoK_{ATP} channels did not exhibit time-depen-

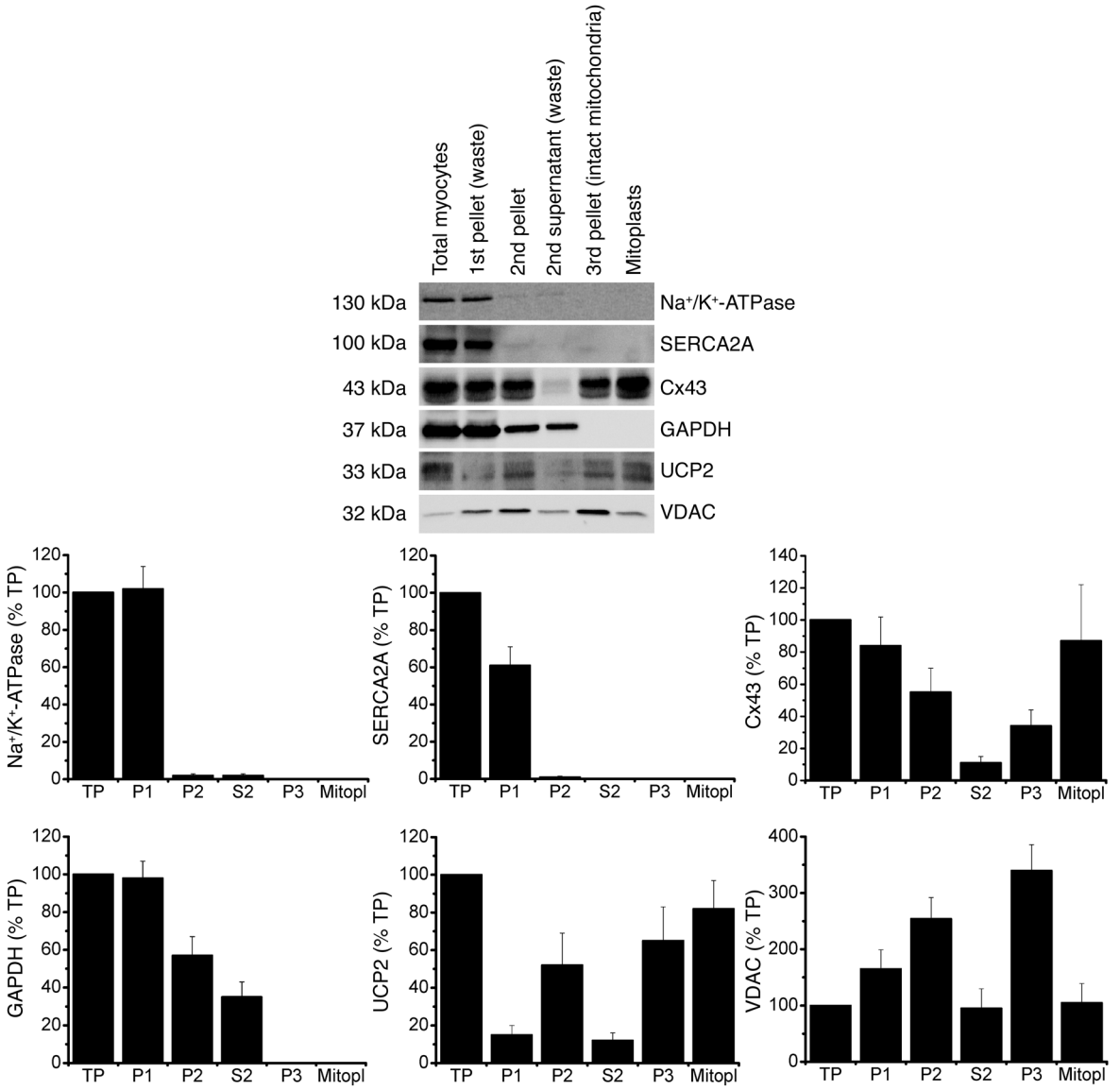

Figure 1

Cx43 is present in isolated subsarcolemmal mitoplasts. Mitochondria were prepared by differential centrifugation as described in Methods. An equal amount of protein (30 μg) from distinct isolation fractions — i.e., crude homogenate of isolated myocytes (TP), first pellet with cell debris (P1, discarded), second pellet containing mitochondria (P2), second supernatant (S2, discarded), intact mitochondria (P3), mitoplasts (Mitopl) — was loaded in each lane, and proteins were analyzed by immunoblotting. Immunoreactivity to the following proteins served as markers for cellular compartments: GAPDH (cytosolic marker), Na^+/K^+-ATPase (plasma membrane marker), SERCA2A (endoplasmic reticulum marker), VDAC (outer mitochondrial membrane marker), UCP2 (inner mitochondrial membrane marker).

dent activation or run-down (continuous 9-second pulse: Po,total, 0.28% ± 0.09% and 4.21% ± 0.50% at baseline and under diazoxide, respectively; n = 6). Diazoxide-stimulated mitoK$_{ATP}$ channel activity was inhibited by the nonselective mitoK$_{ATP}$ inhibitor glibenclamide (10 μM; Po,total, 0.35% ± 0.06%, n = 8) (Figure 2A and Table 1), the selective mitoK$_{ATP}$ inhibitor 5-hydroxydecanoic acid (100 μM; Po,total 0.26% ± 0.16%, n = 6), and magnesium adenosine triphosphate (MgATP; 100 μM; Po,total 0.55% ± 0.09%, n = 5). Thus, mitoK$_{ATP}$ channels are present in wild-type mice and exhibit properties similar to those previously reported for rats (13, 14).

To evaluate whether the diazoxide effect on mitoK$_{ATP}$ channel activity might be mediated via ROS, we (a) measured the effect of diazoxide on mitochondrial H_2O_2 production by the Amplex UltraRed assay (15); and (b) performed mitoK$_{ATP}$ channel recordings in the presence of the ROS scavenger *N*-acetyl-L-cysteine (L-NAC) (16, 17). While antimycin A (4 μg/ml), which stimulates ROS formation by inhibiting respiratory complex III, increased the slope of the Amplex UltraRed fluorescence in both mitochondria and mitoplasts; neither the solvent DMSO nor diazoxide (200 μM) altered Amplex UltraRed fluorescence in mitoplasts maintained in our patch-clamp solution (Figure 2, E and F), supporting the hypothesis that under our experimental conditions, diazoxide had no relevant unspecific effect on mitochondrial ROS production (18). Moreover, the ROS scavenger

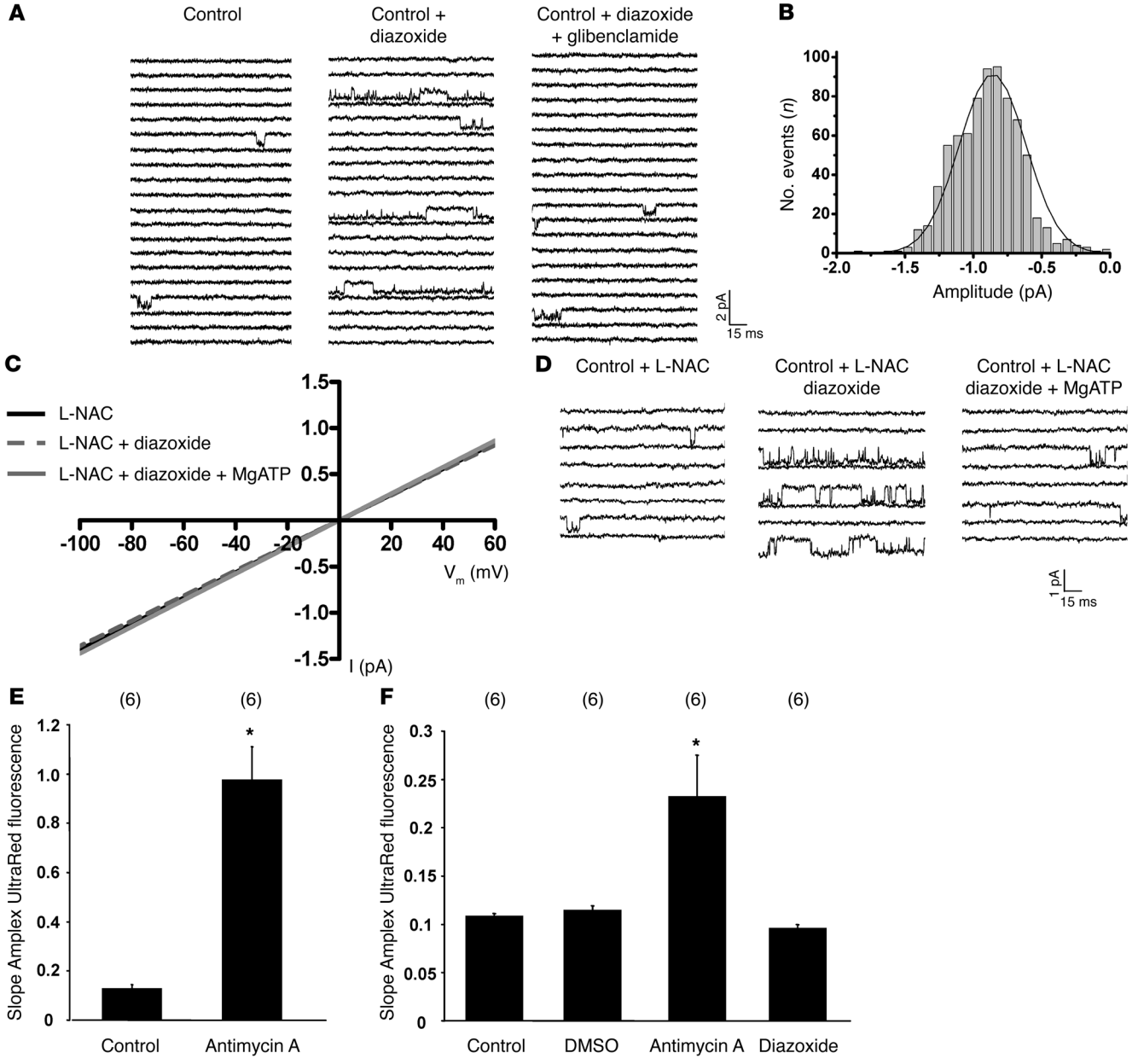

Figure 2

MitoK$_{ATP}$ single-channel activation by diazoxide (100 μM) is independent of ROS. (**A**) Baseline (left) and diazoxide-activated (middle) mitoK$_{ATP}$ currents of wild-type mice in mitoplast-attached configuration at –60 mV, which was blocked by 10 μM glibenclamide (right). (**B**) Amplitude histogram of mitoK$_{ATP}$ current under baseline conditions revealed a mean $I_{unitary}$ of –0.83 ± 0.05 pA (n = 22). V_m, membrane voltage. (**C**) Single-channel amplitude (I) as a function of test potentials. Slope conductances determined by linear regression in individual experiments on wild-type mice were unaffected by the ROS scavenger L-NAC (5 mM) with or without diazoxide and with or without MgATP (100 μM) compared with control (see Figure 3B). (**D**) Baseline single-channel properties (left), the diazoxide effect on mitoK$_{ATP}$ channel activity (middle), and channel inhibition by MgATP (right) (at –60 mV) were unaffected by L-NAC compared with control (**A**). (**E**) Slope of Amplex UltraRed fluorescence of intact mitochondria (10 μg protein) in incubation buffer was significantly increased by the addition of antimycin A; n = 6, *P < 0.05 versus control. (**F**) Slope of Amplex UltraRed fluorescence of mitoplasts (50 μg protein) in patch-clamp buffer was increased by antimycin A but remained unchanged upon addition of the solvent DMSO or diazoxide; n = 6, *P < 0.05 versus control.

L-NAC (5 mM) did no alter baseline mitoK$_{ATP}$ channel properties and, notably, did not attenuate diazoxide-induced mitoK$_{ATP}$ channel activation (Figure 2, C and D, and Table 1), indicating that the stimulation of mitoK$_{ATP}$ channels by diazoxide is not mediated through ROS.

Since Cx43 is found in the inner mitochondrial membrane (Figure 1) (10, 12) and ischemic or pharmacological preconditioning is undermined by Cx43 deficiency independent of cell-cell coupling by gap junctions (11), we aimed to determine whether mitochondrial Cx43 might be an essential molecular component of the

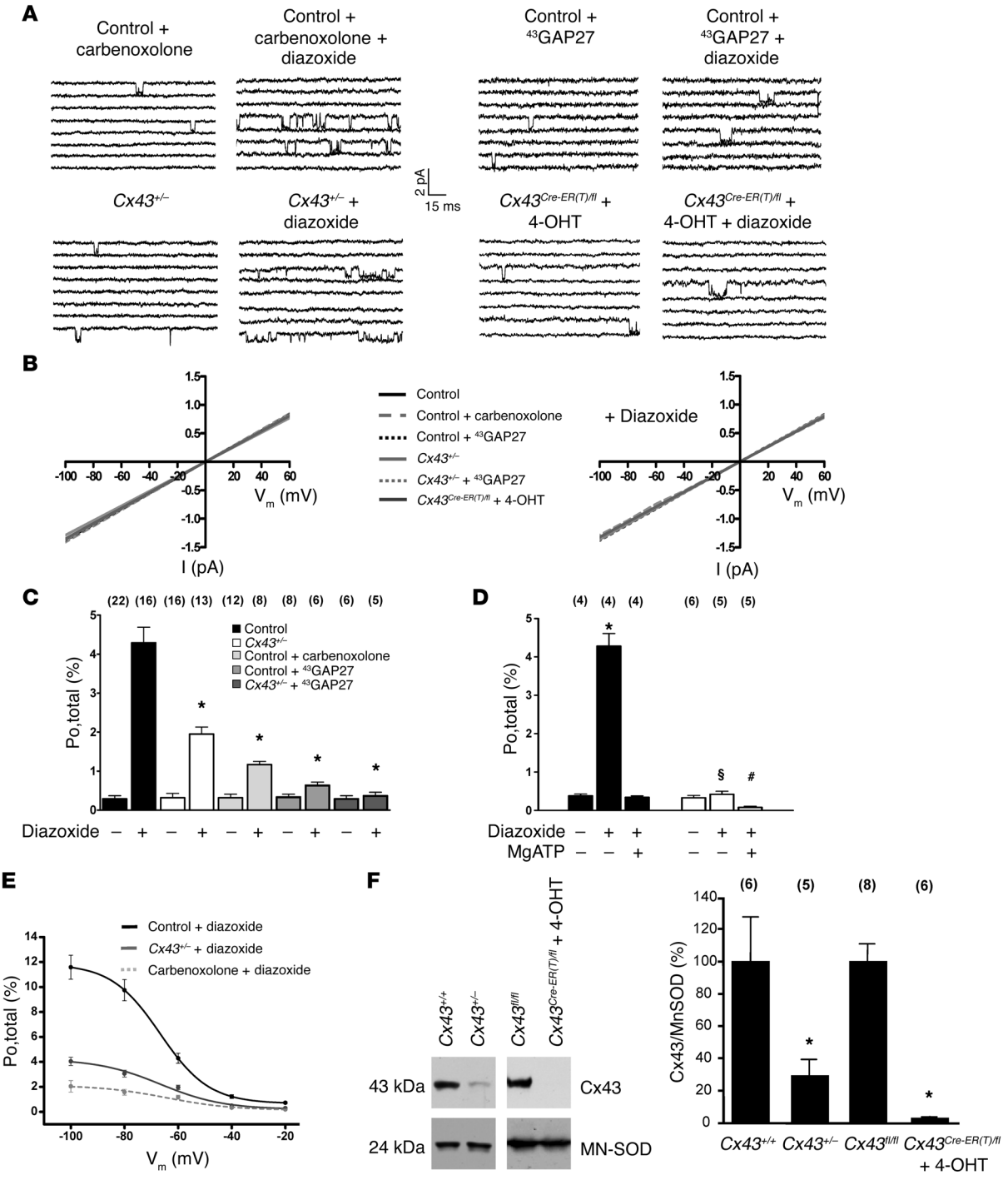

Figure 3

MitoK_{ATP} single-channel activation by diazoxide (100 μM) is dependent on the presence of mitochondrial Cx43. (**A**) The diazoxide effect on mitoK_{ATP} channel activity (at –60 mV) was reduced in wild-type mice by carbenoxolone (10 μM) (upper left) and ^{43}GAP27 (250 μM) (upper right); in *Cx43*$^{+/–}$ mice (lower left); and in *Cx43*$^{Cre\text{-}ER(T)/fl}$ + 4-OHT mice (lower right) compared with control (Figure 2A). (**B**) Single-channel amplitude as a function of test potentials in the absence (left) and presence (right) of diazoxide. Slope conductances were similar in all groups. (**C**) Mean values of the open probability (Po,total) in control, *Cx43*$^{+/–}$ mice, wild-type + carbenoxolone, wild-type + ^{43}GAP27, and *Cx43*$^{+/–}$ mice + ^{43}GAP27 in the absence and presence of diazoxide, as indicated; *n* values are shown in parentheses. **P* < 0.05 versus control. (**D**) Mean values of the open probability (Po,total) in *Cx43*$^{fl/fl}$ control mice (black) and *Cx43*$^{Cre\text{-}ER(T)/fl}$ + 4-OHT mice (white) in the absence and presence of diazoxide and MgATP, as indicated; *n* values are shown in parentheses. **P* < 0.05 versus *Cx43*$^{fl/fl}$ control; §*P* < 0.05 versus *Cx43*$^{fl/fl}$ control + diazoxide; $^{\#}$*P* < 0.05 versus *Cx43*$^{Cre\text{-}ER(T)/fl}$ + 4-OHT. (**E**) Effect of various voltages on diazoxide-stimulated mitoK_{ATP} open probability (Po,total) in control, wild-type + carbenoxolone, and *Cx43*$^{+/–}$ mice. (**F**) Western blot analysis of Cx43 and MN-SOD protein level in mitochondria from *Cx43*$^{+/+}$ control mice, *Cx43*$^{+/–}$ mice, *Cx43*$^{fl/fl}$ control mice, and *Cx43*$^{Cre\text{-}ER(T)/fl}$ + 4-OHT mice. Bar graphs represent ratios of mitochondrial Cx43 level normalized to MN-SOD; *n* values are shown in parentheses. **P* < 0.05 versus control.

Table 1
Gating parameters of mitoK$_{ATP}$ channels and effects of diazoxide, L-NAC, glibenclamide, and MgATP on mitoK$_{ATP}$ single-channel behavior in wild-type mice in the absence or presence of carbenoxolone

Gating parameter	Control	Control + diazoxide	Control + diazoxide + glibenclamide	Control + L-NAC	Control + L-NAC + diazoxide	Control + L-NAC + diazoxide + MgATP	Carbenoxolone	Carbenoxolone + diazoxide	Carbenoxolone + diazoxide + glibenclamide
Po,total (%)	0.29 ± 0.08	4.29 ± 0.40[A]	0.35 ± 0.06[B]	0.35 ± 0.07	3.93 ± 0.41[A,C]	0.38 ± 0.04[D]	0.32 ± 0.09	1.17 ± 0.08[B,E]	0.23 ± 0.07
Availability (%)	21.10 ± 3.04	31.35 ± 2.32[A]	20.79 ± 1.23[B]	23.63 ± 3.13	32.06 ± 2.59[A,C]	21.58 ± 1.25[D]	20.53 ± 1.72	25.08 ± 2.52[B,E]	17.91 ± 2.73
Po,active (%)	1.47 ± 0.19	13.78 ± 0.92[A]	1.71 ± 0.11[B]	1.48 ± 0.14	12.18 ± 0.42[A,C]	1.73 ± 0.13[D]	1.42 ± 0.22	4.97 ± 0.47[B,E]	1.25 ± 0.38
I_{peak} (fA)	32.3 ± 9.30	99.5 ± 8.45[A]	42.6 ± 7.97[B]	35.8 ± 4.91	102.6 ± 6.72[A,C]	40.7 ± 3.25[D]	31.24 ± 3.53	45.33 ± 6.40[B,E]	25.48 ± 7.28
Mean open time (ms)	1.45 ± 0.21	2.57 ± 0.13[A]	1.69 ± 0.21[B]	1.49 ± 0.16	2.54 ± 0.11[A,C]	1.70 ± 0.13[D]	1.52 ± 0.21	1.89 ± 0.18[B,E]	1.31 ± 0.15
Mean closed time (ms)	5.65 ± 0.99	2.46 ± 0.32[A]	5.61 ± 1.43[B]	5.18 ± 0.62	2.44 ± 0.14[A,C]	4.84 ± 0.36[D]	5.12 ± 1.07	4.36 ± 0.62[B]	5.47 ± 0.89
Mean first latency (ms)	64.68 ± 4.26	39.71 ± 2.95[A]	54.57 ± 3.94[B]	62.74 ± 4.18	40.52 ± 2.06[A,C]	57.39 ± 1.55[D]	68.18 ± 5.43	50.12 ± 3.03[B,E]	69.31 ± 4.79
τ_{open} (ms)	0.46 ± 0.07	0.66 ± 0.06[A]	0.42 ± 0.04[B]	0.44 ± 0.4	0.64 ± 0.03[A,C]	0.42 ± 0.04[D]	0.41 ± 0.06	0.59 ± 0.09[E]	0.38 ± 0.08
	(n = 14)	(n = 12)	(n = 7)	(n = 4)	(n = 4)	(n = 4)	(n = 9)	(n = 7)	(n = 7)
$\tau_{closed,\ fast}$ (ms)	0.49 ± 0.06	0.45 ± 0.03	0.47 ± 0.05	0.51 ± 0.03	0.40 ± 0.04[C]	0.47 ± 0.04	0.54 ± 0.07	0.45 ± 0.09	0.48 ± 0.07
	(n = 10)	(n = 8)	(n = 5)	(n = 4)	(n = 4)	(n = 4)	(n = 6)	(n = 5)	(n = 5)
$\tau_{closed,\ slow}$ (ms)	42.40 ± 3.28	16.76 ± 5.71[A]	38.19 ± 3.34[B]	36.29 ± 4.05	17.51 ± 1.79[A,C]	28.33 ± 4.02[D]	24.07 ± 6.04	14.24 ± 2.94[E]	23.02 ± 3.46
	(n = 10)	(n = 8)	(n = 5)	(n = 4)	(n = 4)	(n = 4)	(n = 6)	(n = 5)	(n = 5)
Amplitude/$I_{unitary}$ (pA)	–0.83 ± 0.05	–0.88 ± 0.06	–0.85 ± 0.03	–0.86 ± 0.05	–0.87 ± 0.04	–0.83 ± 0.03	–0.85 ± 0.03	–0.86 ± 0.05	–0.88 ± 0.04
No. experiments	22	16	8	5	5	4	12	8	4

Diazoxide: 100 μM; L-NAC: 5 mM; glibenclamide: 10 μM; MgATP: 100 μM; carbenoxolone: 10 μM. Holding potential, –40 mV; test potential, –60 mV. [A]$P < 0.05$ versus control. [B]$P < 0.05$ versus control + diazoxide. [C]$P < 0.05$ versus control + L-NAC. [D]$P < 0.05$ versus control + L-NAC + diazoxide. [E]$P < 0.05$ versus carbenoxolone.

conducting pore of mitoK$_{ATP}$ channels or might transfer cytoprotective signaling to these channels. To define the role of mitochondrial Cx43, we used 4 complementary approaches, i.e., single-channel recordings of: wild-type mitoplasts in the presence of (a) the connexin inhibitor carbenoxolone (10 μM) (19) and (b) the Cx43 mimetic peptide ^{43}GAP27 (250 μM) (20); and mitoplasts from (c) heterozygous Cx43-deficient (*Cx43*$^{+/-}$) mice (10) and (d) conditional Cx43-deficient mice (4-hydroxytamoxifen–treated [4-OHT–treated] *Cx43*$^{Cre\text{-}ER(T)/fl}$ mice) (21), which have a more pronounced mitochondrial Cx43 knockdown compared with heterozygous *Cx43*$^{+/-}$ mice (Cx43 content in *Cx43*$^{+/-}$ mitochondria, 28.9% ± 9.4% of wild-type; in *Cx43*$^{Cre\text{-}ER(T)/fl}$ + 4-OHT, 2.8% ± 1.1% of *Cx43*$^{fl/fl}$ control; Figure 3F), while circumventing direct or indirect compensation of Cx43 deficiency during development. In all these 4 conditions, mitoK$_{ATP}$ currents were observed with unitary conductance and baseline single-channel characteristics similar to unstimulated recordings of wild-type mitoplasts without Cx43 inhibition (Figure 3, A–D, and Tables 1, 2, and 3). However, carbenoxolone, ^{43}GAP27, and Cx43 deficiency in *Cx43*$^{+/-}$ and *Cx43*$^{Cre\text{-}ER(T)/fl}$ + 4-OHT mice significantly attenuated mitoK$_{ATP}$ stimulation by diazoxide (Figure 3, A–E, and Tables 1–3), indicating that the effect of diazoxide on mitoK$_{ATP}$ channels is mediated via Cx43. This notion was further supported by an additive effect of ^{43}GAP27 with the genetic Cx43 knockdown, i.e., the Cx43 mimetic peptide abolished diazoxide-mediated K$_{ATP}$ channel activation in *Cx43*$^{+/-}$ mice (Figure 3C and Table 2). Inhibition of mitoK$_{ATP}$ channels by MgATP (*Cx43*$^{+/-}$ Po,total, 0.27% ± 0.09%, n = 4) and glibenclamide was retained in the presence of carbenoxolone or ^{43}GAP27 in *Cx43*$^{+/-}$ mice and in *Cx43*$^{Cre\text{-}ER(T)/fl}$ + 4-OHT mice (Figure 3D and Tables 1–3).

To test whether diazoxide sensitivity of mitoK$_{ATP}$ channels might be rescued by an increased mitochondrial Cx43 content in heterozygous *Cx43*$^{+/-}$ mice, we compared Cx43 protein levels and diazoxide-induced mitoK$_{ATP}$ channel activation in mitochondria from the anterior myocardial wall (AW) subjected to IP (by 10 minutes ischemia and 10 minutes reperfusion) with mitochondria from the posterior myocardial wall (PW; no IP) of the same animals. Consistent with previous reports, IP increased mitochondrial Cx43 levels in the AW versus PW (Figure 4A) (10), which was accompanied by significantly more pronounced diazoxide-mediated mitoK$_{ATP}$ channel stimulation (Figure 4, B–E), further supporting the hypothesis that Cx43 affects drug-induced mitoK$_{ATP}$ channel activity.

Activation of PKCε was implicated in cytoprotection conferred by stimulating G protein–linked receptors, because direct activation of the kinase could mimic preconditioning and inhibitors eliminated protection induced by receptor stimulation (22). Given that sarcolemmal Cx43 is a target of PKCε (23) and PKCε is constitutively localized in mitochondria (24), we reasoned that mitoK$_{ATP}$ channels might be activated by mitochondrial PKCε and that this effect might be mediated by mitochondrial Cx43. Thus, we analyzed the effect of PKC activation by PMA (2 μM) and the selective PKCε peptide agonist ψε receptor for activated C kinase (ψεRACK) (0.5 μM) on mitoK$_{ATP}$ single-channels in wild-type and *Cx43*$^{+/-}$ mice. The PKC activa-

Table 2
Gating parameters of mitoK$_{ATP}$ channels and effect of the Cx43 mimetic peptide ^{43}GAP27 (250 μM) on mitoK$_{ATP}$ single-channel behavior in wild-type and *Cx43*$^{+/-}$ mice

Gating parameter	*Cx43*$^{+/-}$	*Cx43*$^{+/-}$ + diazoxide	*Cx43*$^{+/-}$ + diazoxide + glibenclamide	Control + ^{43}GAP27	Control + ^{43}GAP27 + diazoxide	Control + ^{43}GAP27 + diazoxide + MgATP	*Cx43*$^{+/-}$ + ^{43}GAP27	*Cx43*$^{+/-}$ + ^{43}GAP27 + diazoxide	*Cx43*$^{+/-}$ + ^{43}GAP27 + diazoxide + MgATP
Po,total (%)	0.32 ± 0.11	1.95 ± 0.18^{A,B}	0.55 ± 0.06	0.34 ± 0.07	0.64 ± 0.08^{A,C}	0.16 ± 0.06^{C}	0.29 ± 0.08	0.37 ± 0.09^{A}	0.05 ± 0.01^{D}
Availability (%)	20.85 ± 2.91	31.69 ± 1.60^{B}	24.46 ± 2.60	22.54 ± 2.75	19.94 ± 2.21^{A}	18.86 ± 3.35	18.72 ± 4.03	21.40 ± 3.12^{A}	10.17 ± 4.71
Po,active (%)	1.55 ± 0.27	6.06 ± 0.43^{A,B}	1.67 ± 0.13	1.51 ± 0.23	3.18 ± 0.15^{A,C}	1.14 ± 0.12	1.53 ± 0.17	1.76 ± 0.15^{A}	0.46 ± 0.22^{D}
I_{peak} (fA)	29.43 ± 4.8	68.65 ± 9.37^{A,B}	30.84 ± 5.64	36.9 ± 8.24	39.4 ± 4.51^{A}	27.5 ± 5.31	32.7 ± 6.83	51.6 ± 7.46^{A,D}	8.9 ± 5.83^{D}
Mean open time (ms)	1.46 ± 0.17	1.91 ± 0.13^{A,B}	1.61 ± 0.11	1.48 ± 0.23	1.79 ± 0.14^{A,C}	1.27 ± 0.17	1.52 ± 0.18	1.64 ± 0.14^{A}	0.39 ± 0.15^{D}
Mean closed time (ms)	4.86 ± 1.66	3.90 ± 0.31^{A}	4.91 ± 1.19	4.32 ± 0.49	3.92 ± 0.54^{A}	5.69 ± 0.58^{C}	4.16 ± 0.35	4.19 ± 0.24^{A}	6.34 ± 0.53^{D}
Mean first latency (ms)	66.45 ± 3.74	48.68 ± 2.32^{B}	62.25 ± 6.18	62.77 ± 5.28	49.57 ± 2.79^{A,C}	71.95 ± 1.43^{C}	64.76 ± 2.74	60.79 ± 3.88^{A}	80.81 ± 4.60^{D}
τ_{open} (ms)	0.52 ± 0.11	0.63 ± 0.04	0.40 ± 0.12	0.42 ± 0.06	0.49 ± 0.05^{A}	0.36 ± 0.03	0.40 ± 0.05	0.45 ± 0.04^{A}	0.24 ± 0.05^{D}
	(*n* = 12)	(*n* = 10)	(*n* = 5)	(*n* = 7)	(*n* = 5)	(*n* = 5)	(*n* = 6)	(*n* = 5)	(*n* = 4)
$\tau_{closed,\ fast}$ (ms)	0.43 ± 0.11	0.42 ± 0.09	0.42 ± 0.03	0.49 ± 0.08	0.43 ± 0.09	0.54 ± 0.07	0.42 ± 0.09	0.44 ± 0.06	0.81 ± 0.06^{D}
	(*n* = 9)	(*n* = 7)	(*n* = 4)	(*n* = 5)	(*n* = 4)	(*n* = 4)	(*n* = 5)	(*n* = 4)	(*n* = 4)
$\tau_{closed,\ slow}$ (ms)	20.15 ± 5.90	16.12 ± 8.77	19.50 ± 4.83	28.28 ± 5.21	15.07 ± 6.97^{A,C}	23.02 ± 4.09	25.74 ± 3.73	17.96 ± 2.96	22.21 ± 4.15
	(*n* = 9)	(*n* = 7)	(*n* = 4)	(*n* = 5)	(*n* = 4)	(*n* = 4)	(*n* = 5)	(*n* = 4)	(*n* = 4)
Amplitude/$I_{unitary}$ (pA)	–0.84 ± 0.03	–0.87 ± 0.05	–0.86 ± 0.04	–0.84 ± 0.04	–0.82 ± 0.05	–0.84 ± 0.07	–0.85 ± 0.06	–0.83 ± 0.05	–0.83 ± 0.05
No. experiments	16	13	5	8	6	5	6	5	4

MitoK$_{ATP}$ channel stimulation with diazoxide (100 μM) and inhibition with glibenclamide (10 μM) or MgATP (100 μM). Holding potential, –40 mV; test potential, –60 mV. $^{A}P < 0.05$ versus control + diazoxide (Table 1). $^{B}P < 0.05$ versus *Cx43*$^{+/-}$. $^{C}P < 0.05$ versus control + ^{43}GAP27. $^{D}P < 0.05$ versus *Cx43*$^{+/-}$ + ^{43}GAP27.

tor PMA but not its inactive analog 4α-PMA (2 μM) significantly increased mitoK$_{ATP}$ channel activity (Figure 5, A and B, and Table 4). Similarly, selective stimulation of PKCε by ψεRACK enhanced mitoK$_{ATP}$ channel open probability, mean open time, and availability (Figure 5, D and E, and Table 4), while both PMA and ψεRACK resulted in significantly diminished activation of mitoK$_{ATP}$ channels in *Cx43*$^{+/-}$ compared with wild-type mice (Figure 5, A, B, D, and E, and Table 4). Moreover, Western blot analysis revealed enhanced phosphorylation of Cx43 at the PKC phosphorylation site Ser368 in mitochondria stimulated with ψεRACK (5 μM) versus control (Figure 4, F–H), consistent with the notion that Cx43 phosphorylation by PKCε serves to facilitate cytoprotective signal transduction to mitoK$_{ATP}$ channels. To further support the interaction of mitochondrial Cx43 and PKCε, we sought to determine whether these two proteins might associate in mitochondrial protein complexes. Immunoprecipitation of Cx43 from isolated mitochondria revealed a signal for PKCε, while immunoprecipitation of PKCε also showed a signal for Cx43 (Figure 5C), indicating a close association of the two proteins. The use of anti-rabbit IgGs for immunoprecipitation did not indicate a coprecipitation of one of the analyzed proteins, excluding unspecific effects.

In cardiomyocytes, two mitochondrial populations exist, i.e., subsarcolemmal mitochondria located beneath the plasma membrane and interfibrillar mitochondria found between myofibrils (25). Recently, interfibrillar mitochondria were shown not to contain any detectable Cx43 (12). Given our observations that Cx43 transfers cytoprotective signaling to mitoK$_{ATP}$ channels, we therefore reasoned that drug- and PKC-mediated mitoK$_{ATP}$ channel stimulation might be restricted to subsarcolemmal mitochondria. Thus, we evaluated mitoK$_{ATP}$ channel characteristics and responsiveness in isolated interfibrillar mitochondria of wild-type mice. MitoK$_{ATP}$ currents could be recorded in interfibrillar mitoplasts with single-channel properties similar to those of subsarcolemmal mitochondria (Figure 6, A–E). However, single-channel activity of mitoK$_{ATP}$ in interfibrillar mitoplasts was completely insensitive to PKC activation by both PMA and diazoxide (Figure 6, A, B, and D). Importantly, baseline activity was inhibited by MgATP and glibenclamide, thus confirming mitoK$_{ATP}$ channel identity (Figure 6, A, B, and D). The absence of mitoK$_{ATP}$ channel responsiveness to PKC and diazoxide stimulation in interfibrillar mitochondria further confirmed the fundamental role of Cx43 for mitoK$_{ATP}$ channel activation and indicates functional compartmentation of mitochondria in cell signaling.

Discussion

Cell protection involves activation of endogenous signaling, which can confer significant resistance to oxidant and other stresses associated with hypoxia/reoxygenation, thus promoting enhanced capacity for cell survival (1–3). Although mitoK$_{ATP}$ channels have convincingly been demonstrated to serve as central effectors of diverse upstream cytoprotective signaling pathways, the actual mitochondrial proteins involved in this process are unknown (1, 5, 6, 8). Our results provide the first functional evidence to our knowledge of a mitoK$_{ATP}$ channel complex in native mitochondria by linking Cx43 to mitoK$_{ATP}$ channel opening. While purification of mitochondrial proteins and subsequent reconstitution in artificial lipid bilayers or pro-

Table 3
Effect of diazoxide (100 μM) on mitoK$_{ATP}$ single-channel behavior in *Cx43$^{fl/fl}$* control and *Cx43$^{Cre\text{-}ER(T)/fl}$* + 4-OHT mice

Gating parameter	*Cx43$^{fl/fl}$* control	*Cx43$^{fl/fl}$* control + diazoxide	*Cx43$^{fl/fl}$* control + diazoxide + MgATP	*Cx43$^{Cre\text{-}ER(T)/fl}$* + 4-OHT	*Cx43$^{Cre\text{-}ER(T)/fl}$* + 4-OHT + diazoxide	*Cx43$^{Cre\text{-}ER(T)/fl}$* + 4-OHT + diazoxide + MgATP
Po,total (%)	0.38 ± 0.05	4.28 ± 0.33^{A}	0.34 ± 0.04	0.33 ± 0.06	0.42 ± 0.08^{B}	0.08 ± 0.03^{C}
Availability (%)	24.84 ± 2.48	35.66 ± 2.31^{A}	20.44 ± 1.72	22.43 ± 1.96	25.93 ± 2.61^{B}	12.06 ± 1.89^{C}
Po,active (%)	1.50 ± 0.11	12.31 ± 0.59^{A}	1.52 ± 0.13	1.43 ± 0.12	1.60 ± 0.16^{B}	0.51 ± 0.10^{C}
I_{peak} (fA)	36.3 ± 4.07	108.5 ± 5.87^{A}	37.1 ± 3.08	33.2 ± 3.74	39.5 ± 5.04^{B}	11.7 ± 2.83^{C}
Mean open time (ms)	1.52 ± 0.15	2.61 ± 0.18^{A}	1.62 ± 0.21	1.46 ± 0.13	1.56 ± 0.14^{B}	0.65 ± 0.13^{C}
Mean closed time (ms)	4.88 ± 0.52	2.49 ± 0.18^{A}	5.22 ± 0.52	5.63 ± 0.54	4.67 ± 0.78^{B}	7.62 ± 0.43^{C}
Mean first latency (ms)	63.34 ± 4.88	36.80 ± 2.38^{A}	59.18 ± 3.51	63.47 ± 5.01	59.63 ± 3.83^{B}	75.67 ± 2.72^{C}
τ_{open} (ms)	0.43 ± 0.3 (n = 3)	0.67 ± 0.5^{A} (n = 3)	0.41 ± 0.4 (n = 3)	0.44 ± 0.3 (n = 5)	0.46 ± 0.4^{B} (n = 4)	0.24 ± 0.5^{C} (n = 4)
$\tau_{closed,\ fast}$ (ms)	0.48 ± 0.04 (n = 4)	0.41 ± 0.03 (n = 3)	0.47 ± 0.03 (n = 3)	0.49 ± 0.04 (n = 4)	0.47 ± 0.03^{B} (n = 4)	0.78 ± 0.03^{C} (n = 4)
$\tau_{closed,\ slow}$ (ms)	35.41 ± 4.45 (n = 4)	16.99 ± 1.61^{A} (n = 3)	36.18 ± 2.67 (n = 3)	37.23 ± 3.96 (n = 4)	34.12 ± 2.80^{B} (n = 4)	45.36 ± 3.07^{C} (n = 4)
Amplitude/$I_{unitary}$ (pA)	–0.86 ± 0.04	–0.84 ± 0.03	–0.85 ± 0.05	–0.83 ± 0.04	–0.85 ± 0.05	–0.82 ± 0.04
No. experiments	4	4	4	6	5	5

MitoK$_{ATP}$ channel inhibition with MgATP (100 μM). Holding potential, –40 mV; test potential, –60 mV. $^{A}P < 0.05$ versus *Cx43$^{fl/fl}$* control. $^{B}P < 0.05$ versus *Cx43$^{fl/fl}$* control + diazoxide. $^{C}P < 0.05$ versus *Cx43$^{Cre\text{-}ER(T)/fl}$* + 4-OHT + diazoxide.

teosomes suggested that mitoK$_{ATP}$ channels are incorporated in a multiprotein complex (26, 27), this process may be compromised by unspecific contamination, and protein association does not necessarily reflect functional interaction in native tissue. Moreover, specification of copurified proteins was largely based on immunoreactivity without detailed proteomic analysis, which bears the uncertainty of false-positive antibody cross-binding to unrelated proteins (8, 27). In the present study, we aimed to circumvent these limitations and show in isolated mitoplasts by a pharmacological, a peptide mimetic, and a genetic approach that Cx43 plays a key role in diazoxide- and PKC-induced mitoK$_{ATP}$ channel stimulation, thus defining what we believe to be a novel functional role for Cx43.

Beyond cell-cell coupling, connexin hexamers, monomers, and C-terminal fragments are involved in cell signaling (28, 29). Our observation that carbenoxolone, which inhibits gap junctions and connexin hexamers (19), suppressed mitoK$_{ATP}$ channel activation similarly to genetic Cx43 deficiency suggests that Cx43 in mitochondria forms hemichannels. While such hemichannels may conduct potassium and may be modulated by ATP (30), the presence of mitoK$_{ATP}$ channels in interfibrillar mitochondria lacking Cx43 argues against the notion that Cx43 builds the conduction pore of mitoK$_{ATP}$ channels. Existence of a channel pore that is distinct from Cx43 is further supported by the lower single-channel conductance of mitoK$_{ATP}$ channels than reported for full and subconductance states of connexons and gap junctions (31). Rather, our results demonstrate that Cx43 is essential for cytoprotective signal transduction on mitoK$_{ATP}$ channels, which is supported 7-fold, i.e., by reduced responsiveness of these channels in the presence of (a) pharmacological Cx43 inhibition, (b) Cx43 mimetic peptides, (c) genetic heterozygous Cx43 suppression, (d) almost complete Cx43 reduction in conditional genetic Cx43 knockdown mice, (e) additive effects of ^{43}GAP27 with the genetic *Cx43$^{+/-}$* suppression, (f) rescue of diazoxide sensitivity in *Cx43$^{+/-}$* mice upon IP-induced Cx43 increase, and (g) absence of diazoxide/PKC response in interfibrillar mitochondria lacking Cx43.

In vivo and single-cell studies showed that both Cx43 and PKCε translocate to mitochondria during IP and are pivotal components of preconditioning (7, 10, 22). While the present experiments confirm an IP-mediated increase in mitochondrial Cx43, our results now in addition provide a functional link between these two proteins, with PKCε phosphorylating mitochondrial Cx43 in vitro and being upstream of Cx43 in cytoprotective signal cascades. Although our experiments may not discriminate whether IP and PKCε induce stimulation of mitoK$_{ATP}$ channels through upregulation of mitochondrial Cx43 alone or additional Cx43 phosphorylation in vivo, our observation of Cx43-mediated mitoK$_{ATP}$ channel regulation suffices to explain previous reports of abolished pharmacological and IP and reduced formation of ROS in *Cx43$^{+/-}$* mice (9–11).

Emerging data indicate that localization of signaling molecules is a key component in cell function (32, 33). Mitochondria are known to be distributed in different subcellular compartments (25). Our data show that responsiveness to cytoprotective signal transduction via PKC and subsequently mitoK$_{ATP}$ channels is restricted to subsarcolemmal mitochondria, which are localized adjacent to the upstream receptors. Conversely, interfibrillar mitochondria do not seem to be involved in these cytoprotective pathways, given the observed diazoxide and PKC insensitivity of their mitoK$_{ATP}$ channels. Thus, our observations extend previous reports of distinct structure and biochemical properties of mitochondrial subgroups (25, 34), now indicating that these subpopulations are assigned to distinct cellular functions and suggesting that cardiac cytoprotection via mitoK$_{ATP}$ channel activation is confined to a circumscribed subsarcolemmal compartment.

Understanding the mechanisms involved in cell protection enhances the expectation that one may pharmacologically intervene to block or modulate cell death. The fact that Cx43 regulates mitoK$_{ATP}$ channel activity in native mitochondria makes Cx43 an attractive target for drug development against ischemic injury.

Table 4
Effect of PKC stimulation with PMA (2 μM) and the epsilon-selective peptide ψεRACK (0.5 μM) on mitoK$_{ATP}$ single-channel behavior in wild-type compared with *Cx43*$^{+/-}$ mice

Gating parameter	Control + PMA	Control + PMA + glibenclamide	*Cx43*$^{+/-}$ + PMA	*Cx43*$^{+/-}$ + PMA + glibenclamide	Control + ψεRACK	Control + ψεRACK + MgATP	*Cx43*$^{+/-}$ + ψεRACK	*Cx43*$^{+/-}$ + ψεRACK + MgATP
Po,total (%)	7.01 ± 0.66^{A}	0.54 ± 0.07^{A,B}	3.73 ± 0.30^{B,C}	0.23 ± 0.11	4.35 ± 0.49 ^{A}	0.55 ± 0.09^{A,D}	2.08 ± 0.11^{C,D}	0.27 ± 0.09
Availability (%)	42.53 ± 6.26^{A}	26.01 ± 4.76^{B}	33.39 ± 2.78^{B,C}	17.01 ± 4.87	34.80 ± 2.87^{A}	25.93 ± 4.80^{D}	28.46 ± 3.25^{C,D}	19.25 ± 2.88
Po,active (%)	16.47 ± 2.43^{A}	2.04 ± 0.13^{B}	11.09 ± 0.78^{B,C}	1.32 ± 0.24	12.42 ± 1.61^{A}	2.10 ± 0.19^{D}	7.31 ± 0.58^{C,D}	1.43 ± 0.15
I_{peak} (fA)	122.89 ± 9.43^{A}	51.42 ± 12.43^{B}	89.67 ± 16.73^{B,C}	26.56 ± 8.91	107.73 ± 15.88^{A}	48.67 ± 7.82^{A,D}	77.52 ± 13.81^{C,D}	28.78 ± 6.73
Mean open time (ms)	2.69 ± 0.23^{A}	1.78 ± 0.17^{AB}	2.16 ± 0.21^{B,C}	1.29 ± 0.15	2.32 ± 0.19^{A}	1.72 ± 0.12^{A,D}	1.93 ± 0.16 ^{C,D}	1.24 ± 0.17
Mean closed time (ms)	2.01 ± 0.32^{A}	3.41 ± 1.23^{B}	3.02 ± 0.49^{B}	5.89 ± 0.32	2.81 ± 0.29^{A}	4.06 ± 0.71^{A,D}	3.54 ± 0.19^{D}	6.57 ± 0.27
Mean first latency (ms)	31.73 ± 3.63^{A}	53.79 ± 2.51^{AB}	50.62 ± 3.37^{B,C}	68.95 ± 2.22	40.97 ± 2.57^{A}	54.22 ± 2.93^{A,D}	53.70 ± 2.63^{C,D}	65.63 ± 3.25
τ_{open} (ms)	0.62 ± 0.05^{A}	0.39 ± 0.09^{B}	0.57 ± 0.04	0.41 ± 0.03	0.61 ± 0.03^{A}	0.38 ± 0.08^{D}	0.53 ± 0.05^{C,D}	0.40 ± 0.05
	(*n* = 4)	(*n* = 4)	(*n* = 4)	(*n* = 4)	(*n* = 5)	(*n* = 4)	(*n* = 5)	(*n* = 4)
$\tau_{shut,\ fast}$ (ms)	0.34 ± 0.06^{A}	0.48 ± 0.04^{B}	0.44 ± 0.08^{B}	0.51 ± 0.07	0.37 ± 0.03^{A}	0.51 ± 0.06^{D}	0.45 ± 0.07	0.56 ± 0.03
	(*n* = 4)	(*n* = 4)	(*n* = 4)	(*n* = 4)	(*n* = 4)	(*n* = 4)	(*n* = 4)	(*n* = 4)
$\tau_{shut,\ slow}$ (ms)	9.37 ± 3.86^{A}	25.03 ± 2.37^{A,B}	27.99 ± 3.42	31.72 ± 3.28	17.44 ± 2.82^{A}	23.87 ± 2.28^{A,D}	31.35 ± 2.77^{C,D}	30.03 ± 4.14
	(*n* = 4)	(*n* = 4)	(*n* = 4)	(*n* = 4)	(*n* = 4)	(*n* = 4)	(*n* = 4)	(*n* = 4)
Amplitude/$I_{unitary}$ (pA)	–0.87 ± 0.04	–0.88 ± 0.07	–0.88 ± 0.04	–0.86 ± 0.05	–0.85 ± 0.06	–0.87 ± 0.02	–0.84 ± 0.05	–0.86 ± 0.05
No. experiments	5	4	6	5	5	5	5	4

MitoK$_{ATP}$ channel inhibition with glibenclamide (10 μM) or MgATP (100 μM). Holding potential, –40 mV; test potential, –60 mV. $^{A}P < 0.05$ versus control. $^{B}P < 0.05$ versus control + PMA. $^{C}P < 0.05$ versus *Cx43*$^{+/-}$. $^{D}P < 0.05$ versus control + ψεRACK.

Methods

The present study was performed with approval by the Bioethical Committee of the Landesamt für Natur, Umwelt und Verbraucherschutz Nordrhein-Westfalen in Recklinghausen and conforms to the NIH *Guide for the care and use of laboratory animals* (publication no. 85-23. Revised 1996).

Mouse hearts. Hearts were obtained from C57BL/6J mice, heterozygous *Cx43*$^{+/-}$ mice (35), and wild-type littermates, as indicated. More complete ablation of Cx43 was induced in adult *Cx43*$^{Cre\text{-}ER(T)/fl}$ mice by the intraperitoneal injection of 3 mg 4-OHT once per day on 5 consecutive days as previously described (10, 21). These animals were sacrificed at day 12 after the first injection. For control, *Cx43*$^{fl/fl}$ mice were used (10, 21).

Preparation of cardiomyocytes and subsarcolemmal/interfibrillar mitoplasts. Single ventricular myocytes were isolated by enzymatic digestion, as previously described (36). Freshly isolated cardiomyocytes were used within 1–2 hours. Myocytes were labeled with Mitotracker Green (1 μM; Molecular Probes, Invitrogen) to facilitate identification of intact mitoplasts after further subcellular purification. Isolated intact subsarcolemmal mitoplasts were prepared from isolated myocytes by differential centrifugation, as previously reported (13, 37–39). Briefly, myocytes were suspended for 30 minutes in a solution containing (in mM) 250 sucrose, 5 K-HEPES, and 1 $CaCl_2$ to rupture the sarcolemma and spun at 1,500 *g* for 10 minutes. The supernatant containing the subsarcolemmal mitochondria was pelleted (8,500 *g*, 10 minutes, 4°C). The mitochondria were further purified by 2 additional centrifugation cycles (8,500 *g*, 10 minutes, 4°C) and the final pellet resuspended in K^+ solution (in mM: 150 KCl, 5 K-HEPES, 1 $CaCl_2$, pH 7.2).

Isolated intact interfibrillar mitoplasts were prepared from isolated murine hearts, as previously described (12). In brief, murine hearts were removed quickly after decapitation and were washed in buffer A (in mM: 100 KCl, 5 $MgSO_4$, 50 3-[*N*-morpholino]-propanesulfonic acid (MOPS), 1 EGTA, 1 MgATP, pH 7.4). The ventricular tissue was minced in 10 ml/g buffer B (buffer A plus 0.04% BSA), homogenized in a Potter-Elvehjem grinder, and spun at 800 *g* for 10 minutes. The pellet containing the interfibrillar mitochondria was resuspended in buffer B, treated for 1 minute with nargase (8 U/g tissue [bacterial, type XXIV, Sigma-Aldrich]), homogenized with a Potter-Elvehjem grinder, and spun at 800 *g* for 10 minutes. The supernatant was further purified by an additional centrifugation cycle (8,000 *g*, 10 minutes, 4°C) and the final pellet resuspended in K^+ solution (in mM: 150 KCl, 5 K-HEPES, 1 $CaCl_2$, pH 7.2). Mitochondria were stored at 4°C for up to 48 hours for patch-clamp experiments. Mitoplasts were prepared from intact mitochondria prior to patching or protein preparation by osmotic shock or digitonin, as previously described (14, 40).

Single-channel recordings. All experiments were performed in the mitoplast-attached configuration of the patch-clamp technique (180 test pulses of 150-ms duration at 1.67 Hz, if not indicated otherwise; sampling frequency, 10 kHz; corner frequency, 2 kHz) with symmetrical bath and pipette solution composed of (in mM): 150 KCl, 10 K-HEPES; pH was adjusted to 7.2 with KOH, as previously described (13, 38). Currents were recorded and digitized with an Axopatch 200B amplifier and Digidata 1200 interface (Axon Instruments) with the use of custom software (CDE-REVL-LEVL/X program, version 1.3) (41, 42).

Single-channel analysis. Single-channel analysis was done using custom software only from 1-channel patches, as previously reported (13, 37, 43, 44). Linear leak and capacity currents were digitally subtracted using the average currents of nonactive sweeps. For detailed gating analysis, idealized currents were analyzed in 150-ms steps (unless otherwise indicated). Active sweeps were defined as those with at least 1 opening. The open probability of active sweeps (Po,active; defined as the occupancy of the open state during active sweeps), the availability (fraction of sweeps containing at least 1 channel opening), and I_{peak} (the peak ensemble

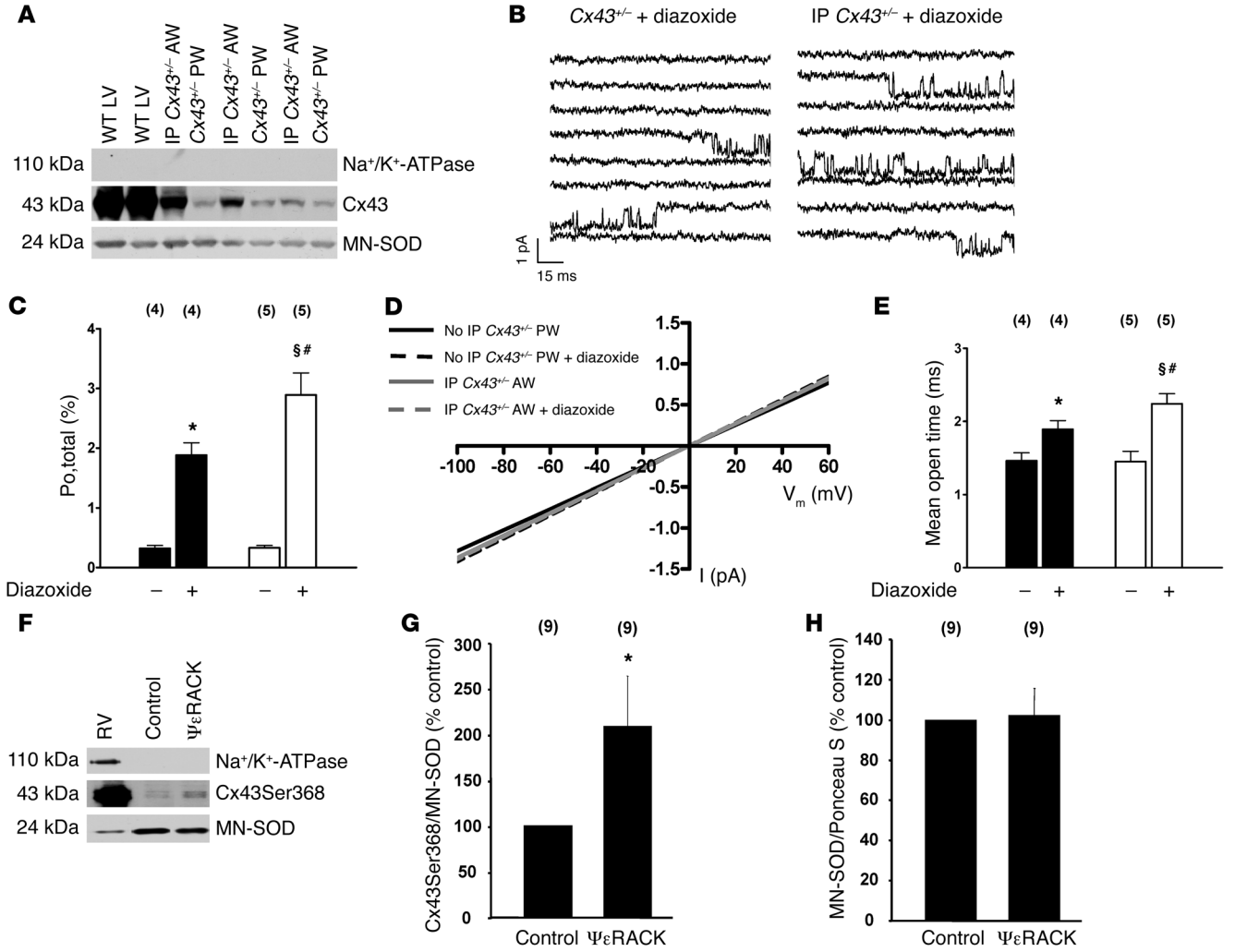

Figure 4

IP increases mitochondrial Cx43 content in *Cx43*$^{+/-}$ mice and rescues diazoxide sensitivity of mitoK$_{ATP}$ channels (**A**–**E**). (**A**) Western blots of Cx43 and MN-SOD in mitochondria from the AW subjected to IP and PW (no IP) of the same *Cx43*$^{+/-}$ mouse (IP-induced Cx43 increase normalized to MN-SOD, 4.0 ± 0.9, $n = 3$). Mitochondrial proteins from wild-type left ventricle (WT LV): positive control; Na^+/K^+-ATPase: exclusion of contamination with sarcolemmal proteins. (**B**) The diazoxide effect on mitoK$_{ATP}$ activity (at –60 mV) in *Cx43*$^{+/-}$ mice was enhanced by IP (right) versus control (left). (**C** and **E**) Mean values of open probability (Po,total) (**C**) and mean open time (**E**) in PW (black) and AW (IP; white) of *Cx43*$^{+/-}$ mice in the absence and presence of diazoxide, as indicated; *n* values are shown in parentheses. (**D**) Single-channel amplitude as a function of test potentials. Slope conductances were similar in PW and AW (subjected to IP) of *Cx43*$^{+/-}$ mice and were unaffected by diazoxide.*$P < 0.05$ versus PW control; §$P < 0.05$ versus AW control; #$P < 0.05$ versus PW + diazoxide. (**F**–**H**) Mitochondrial PKCε phosphorylates mitochondrial Cx43 at Ser368. (**F**) Western blots for phospho-Cx43Ser368 and MN-SOD in mitochondria incubated for 30 minutes under control conditions or with ψεRACK (5 μM). Right ventricular protein (RV): positive control; Na^+/K^+-ATPase: exclusion of contamination with sarcolemmal proteins. (**G**) Ratios of mitochondrial phospho-Cx43Ser368 levels normalized to MN-SOD; *n* values are shown in parentheses. *$P < 0.05$ versus control. (**H**) Ratios of mitochondrial MN-SOD levels normalized to Ponceau S staining to demonstrate the suitability of MN-SOD as a housekeeping protein; *n* values are shown in parentheses.

average current) were calculated at –60 mV (unless otherwise indicated). The total open probability (Po,total; defined as the occupancy of the open state during the total pulse duration) was analyzed for 9-second pulse durations at –60 mV of 180 sweeps with 150-ms duration or, if indicated, of continuous pulses. Single-channel amplitudes were determined by direct measurements of fully resolved openings for conductance calculations or as the maximum of Gaussian fits to amplitude histograms. Time constants of open time (τ_{open}) and closed time histograms (τ_{closed}) were obtained by simplex maximum likelihood estimation on all-level open and closed time distributions.

IP. We used the in situ mouse heart model, as described previously (45, 46). Briefly, *Cx43*$^{+/-}$ mice were anesthetized with pentobarbital sodium (80 mg/kg i.p.). The temperature of the animals was kept stable between 36.6 and 37.4°C using heating pads, and the electrocardiogram was monitored continuously. After intubation (polyethlene-60 tubing), the animals were ventilated with a stroke rate of 130/min and a tidal volume of 1 ml with oxygen-supplemented room air. A midline thoracotomy and pericardiotomy were performed. The left anterior descending coronary artery was occluded 2–3 mm distal to the tip of the left auricle using a 7.0 silk suture and a small tube to form a snare. After 10 minutes occlusion, the hearts

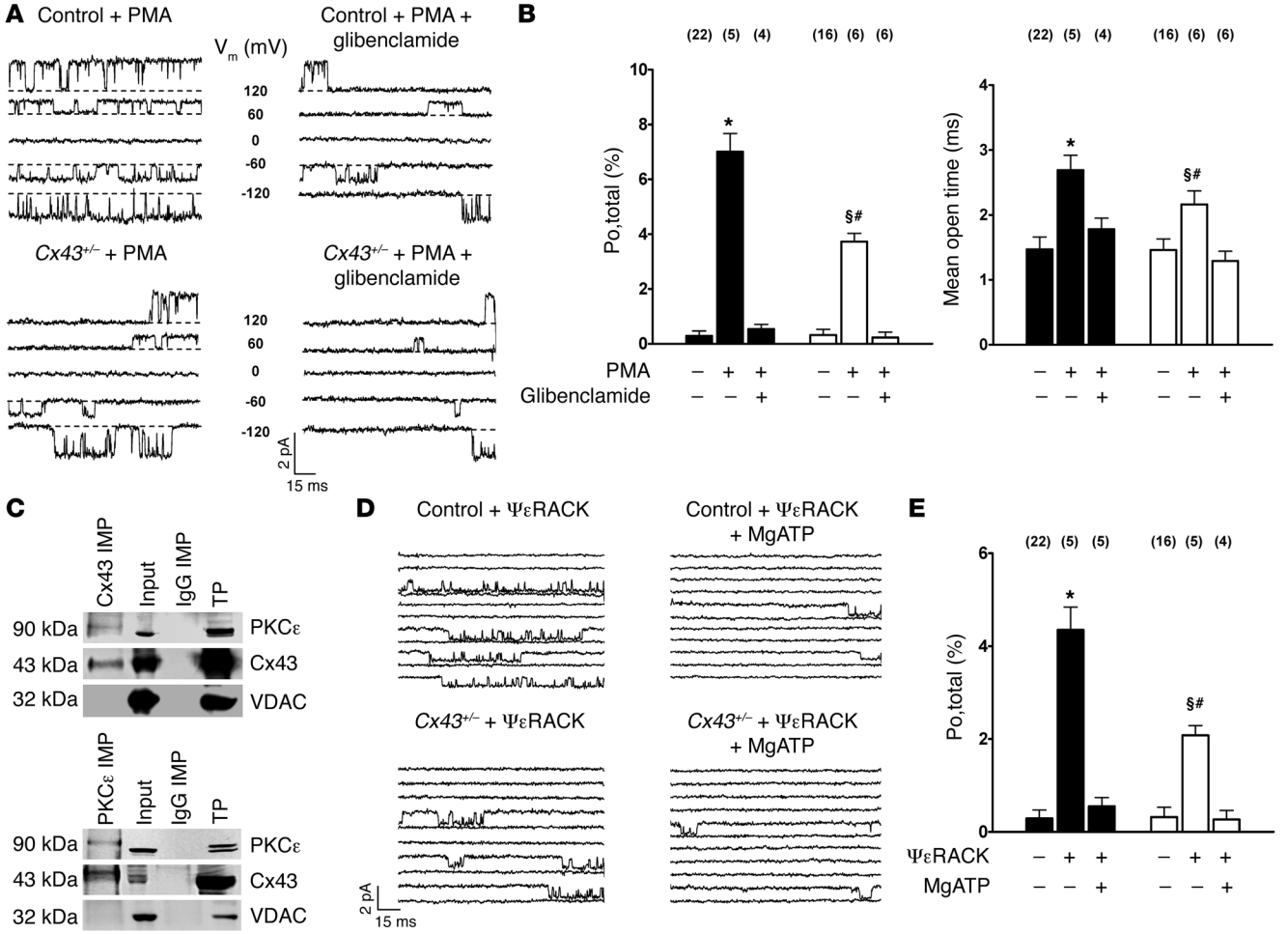

Figure 5

PKC-mediated stimulation of mitoK$_{ATP}$ channel activity is diminished in *Cx43*$^{+/-}$ mice. (**A**) MitoK$_{ATP}$ single-channel activity is activated by PKC stimulation with PMA 2 μM (top left), which can be inhibited by glibenclamide 10 μM (top right). PMA-induced mitoK$_{ATP}$ channel activation is reduced in *Cx43*$^{+/-}$ mice (bottom). Voltages are indicated. (**B**) Mean values of mitoK$_{ATP}$ channel open probability (Po,total; left) and mean open time (right) in control (black) and *Cx43*$^{+/-}$ mice (white) in the absence and presence of PMA and glibenclamide, as indicated; *n* values are shown in parentheses. **P* < 0.05 versus control; §*P* < 0.05 versus *Cx43*$^{+/-}$; #*P* < 0.05 versus control + PMA. (**C**) Proteins of mitochondria were immunoprecipitated (IMP) for Cx43 (top) or PKCε (bottom). Western blot analysis for coprecipitated Cx43 and PKCε revealed positive results. Precipitation of mitochondrial proteins with anti-rabbit IgGs was used as negative control. Input lysates and a total ventricular protein extract (TP) were analyzed as positive control. Immunoblotting against VDAC was performed to exclude any unspecific coimmunoprecipitation. (**D**) MitoK$_{ATP}$ single-channel activity was activated by selective PKCε stimulation with ψεRACK (top left), which could be inhibited by MgATP (top right). ψεRACK-induced mitoK$_{ATP}$ channel activation was reduced in *Cx43*$^{+/-}$ mice (bottom). (**E**) Mean values of mitoK$_{ATP}$ channel open probability in control (Po,total; black) and *Cx43*$^{+/-}$ mice (white) in the absence and presence of the selective PKCε peptide agonist ψεRACK (0.5 μM) and MgATP (100 μM), as indicated; *n* values are shown in parentheses. **P* < 0.05 versus control; §*P* < 0.05 versus *Cx43*$^{+/-}$; #*P* < 0.05 versus control + ψεRACK.

were reperfused for 10 minutes. At the end of the protocol, hearts were rapidly excised, the anterior and posterior walls were separated, and mitochondria or mitoplasts were isolated as described above (*n* = 3).

Western blot analysis. Mitochondria were prepared as described above. Proteins were prepared from different isolation fractions (as indicated) with standard methods, as described previously (43). Protein concentration was assayed using a commercial protein assay (BCA method, Pierce). After standard Laemmli SDS-PAGE (12%) and Western blotting (Bio-Rad Tankblot system, nitrocellulose membrane), proteins were detected using the following primary antibodies: Cx43 (1:5,000, rabbit polyclonal, ab11370, Abcam), GAPDH (1:200, rabbit polyclonal IgG, sc-25778, Santa Cruz Biotechnology Inc.), Na^+/K^+-ATPase (1:1,000, rabbit polyclonal IgG, no. 3010, Cell Signaling Technology Inc.), sarcoplasmic reticulum Ca^{2+} pump gene 2 (SERCA2A; 1:100, goat polyclonal IgG, sc-8094, Santa Cruz Biotechnology Inc.), voltage-dependent anion channel (VDAC; 1:1,000, rabbit polyclonal IgG, no. 4866, Cell Signaling Technology Inc.), uncoupling protein 2 (UCP2; 1:100, goat polyclonal IgG, sc-6525, Santa Cruz Biotechnology Inc.), manganese superoxide dismutase (MN-SOD; 1:1,000, rabbit polyclonal IgG, Upstate), Cx43 phosphorylated at serine 368 (Cx43Ser368; 1:500, rabbit polyclonal IgG, Cell Signaling Technology Inc.), and horseradish peroxidase–coupled anti-rabbit secondary antibody (1:2,000, Sigma-Aldrich). Primary antibody incubations were performed overnight at 4°C. Immunoreactive bands were stained with ECL reagents (Amersham Pharmacia Biotech) according to the manufacturer's instructions. Densitometrical analysis of protein induction was performed using a CCD camera (Raytest) with AIDA densitometry analysis software (Raytest). Each Western blot was performed in triplicate, unless otherwise indicated.

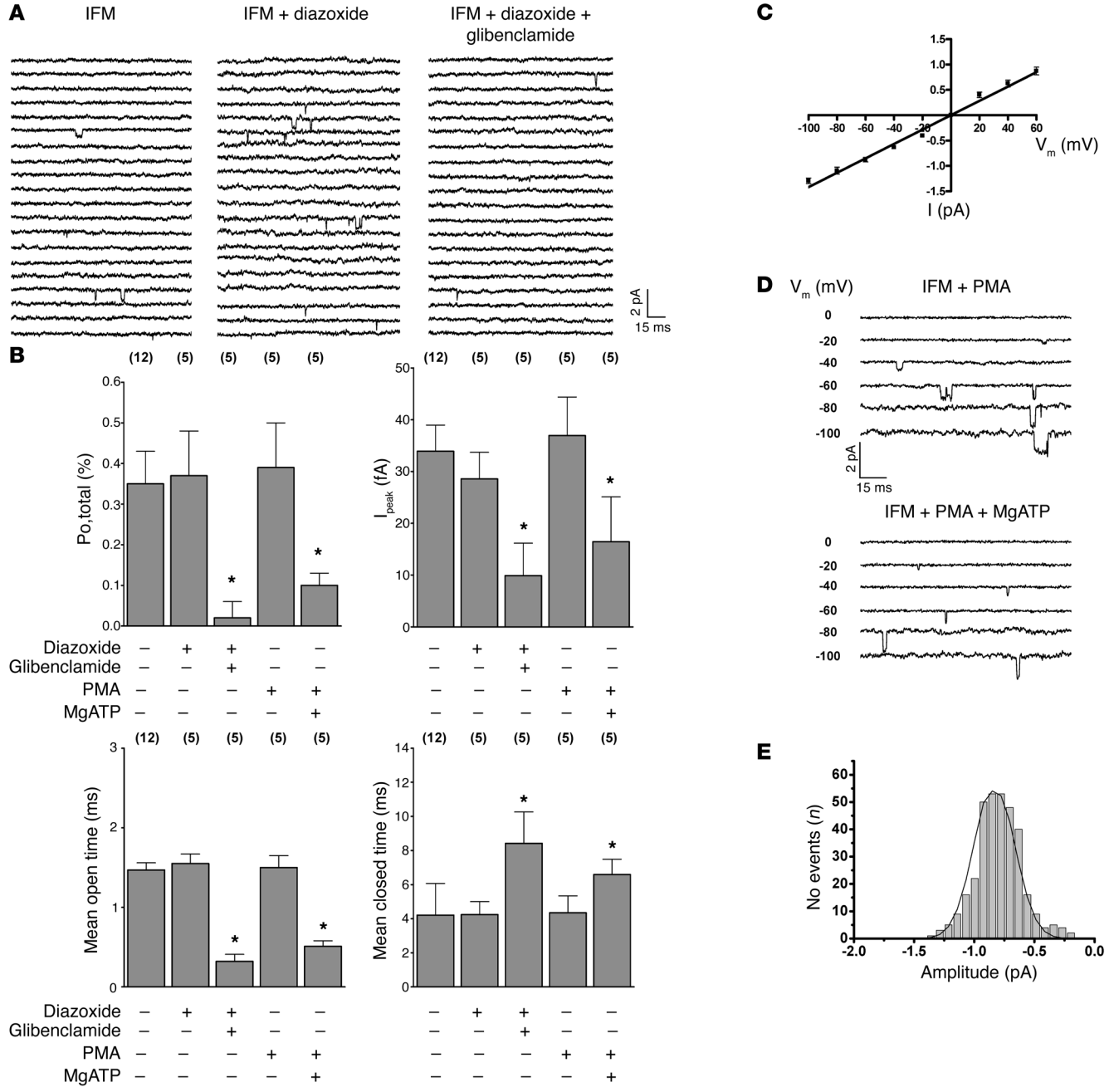

Figure 6

MitoK$_{ATP}$ channel activity of interfibrillar mitochondria is insensitive to PKC and diazoxide (100 μM) stimulation. (**A**) MitoK$_{ATP}$ single-channel current (at –60 mV) of interfibrillar mitochondria (left), which was not activated by diazoxide (middle) but was inhibited by glibenclamide (right). (**B**) Mean values of mitoK$_{ATP}$ channel open probability (Po,total; top left), I_{peak} (top right), mean open time (bottom left), and mean closed time (bottom, right) of interfibrillar mitochondria in the absence and presence of diazoxide, PMA, glibenclamide, and MgATP, as indicated; *n* values are shown in parentheses. **P* < 0.05 versus control. Single-channel amplitude as a function of test potentials. (**C**) Slope conductance (14.1 ± 0.5 pS, *n* = 6) of interfibrillar mitoK$_{ATP}$ channels determined by linear regression in individual experiments was similar to that of subsarcolemmal mitochondria (Figure 3B). (**D**) MitoK$_{ATP}$ single-channel activity of interfibrillar mitochondria (IFM) was not activated by PKC stimulation with 2 μM PMA (top). Baseline activity was inhibited by 100 μM MgATP (bottom). Voltages are indicated. (**E**) Amplitude histogram of interfibrillar mitoK$_{ATP}$ current under baseline conditions revealed a mean $I_{unitary}$ of –0.85 ± 0.04 pA (*n* = 12).

*Immunoprecipitation of Cx43 with PKC*ε. Proteins were prepared from isolated mitochondria. Samples (500 μg of mitochondrial protein) were incubated with anti-PKCε antibody (rabbit polyclonal anti-human, 20 μg, Santa Cruz Biotechnology Inc.), anti-Cx43 antibody (rabbit polyclonal anti-rat total Cx43, 25 μg, Zytomed), or anti-rabbit IgGs before binding to protein A. The beads were washed 3 times with 0.5 ml phosphate-buffered saline. Immunoprecipitated proteins were electrophoretically separated on 10% polyacrylamide gels and subsequently transferred to nitrocel-

lulose membranes. Input lysates and total ventricular protein served as control. Immunoblotting against VDAC (1:1,000, rabbit polyclonal IgG, no. 4866, Cell Signaling Technology Inc.) was performed to exclude any unspecific coimmunoprecipitation. Primary antibody incubations were performed overnight at 4°C. Immunoreactive bands were detected using the SuperSignal West Femto Maximum Sensitivity Substrate (Pierce). Each immunoprecipitation was performed in triplicate.

PKC stimulation and Cx43 phosphorylation. Mitochondria were isolated from the ventricles of male C57BL/6J mice and purified by Percoll gradient ultracentrifugation. Intact mitochondria were stimulated in incubation buffer (in mM: 125 KCl, 10 Tris-MOPS, 1.2 Pi-Tris, 1.2 $MgCl_2$, 0.02 EGTA, 5 glutamate, 2.5 malate, pH 7.4) supplemented with 200 μM ATP for 30 minutes at 25°C with continuous shaking without or with the PKCε-activating peptide ΨεRACK (5 μM). After stimulation, mitochondrial proteins were isolated in 1× cell lysis buffer (containing in mM: 20 Tris pH 7.5, 150 NaCl, 1 EDTA, 1 EGTA, 2.5 sodium pyrophosphate, 1 β-glycerophosphate, 1 Na_3VO_4, 1% Triton X-100, 1 μg/ml leupeptin, supplemented with 1× Complete Protease Inhibitor Cocktail [Roche]). After sonication, the samples were centrifuged at 14,000 *g* for 10 minutes at 4°C. The protein concentration of the supernatant was determined using the Protein Dc Kit (Bio-Rad). Ten micrograms mitochondrial or right-ventricular proteins were subjected to Western blot analysis (see above). Signal intensities of Cx43Ser368 were normalized to the respective MN-SOD signals. MN-SOD immunoreactive signals were also normalized to Ponceau S staining to ensure that MN-SOD was suitable as a reference protein. Signals were quantified using Scion Image software (Scion Corp.).

Measurement of H_2O_2. H_2O_2 generation was measured with Amplex UltraRed (Invitrogen) according to the manufacturer's instructions. In brief, 10 μg intact mitochondria of C57BL/6J mice were incubated with 50 μM Amplex UltraRed and 0.1 U/ml horseradish peroxidase in incubation buffer (in mM: 125 KCl, 10 Tris-MOPS, 1.2 Pi-Tris, 1.2 $MgCl_2$, 0.02 EGTA, 5 glutamate, 2.5 malate, pH 7.4) without or with antimycin A. In addition, H_2O_2 generation was measured from 50 μg mitoplasts in patch-clamp solution without or with antimycin A, diazoxide, or the vehicle DMSO, as indicated. Fluorescence was measured for 10 minutes continuously with a Varian Cary Eclipse spectrophotometer at excitation/emission wavelengths of 565/581 nm. Background fluorescence of the buffer without mitochondria was subtracted, and the slope was calculated.

Materials and statistical analysis. In some experiments, MgATP, diazoxide, glibenclamide, 5-hydroxydecanoic acid, carbenoxolone (19), PMA, 4α-PMA, L-NAC (Sigma-Aldrich), the PKCε-specific activator peptide ψεRACK (HDAPIGYD, synthesized with stated purity >95% by EZBiolab) (7), and/or the Cx43 mimetic peptide ^{43}GAP27 (SRPTEKTIFII, synthesized with stated purity >85% by Eurogentec) (20) were added to the bath solutions, as indicated. Pooled data are presented as mean ± SEM. Comparisons between groups were performed with 1-way ANOVA or 2-tailed Student's *t* test (Cx43 phosphorylation). A *P* value less than 0.05 was considered significant.

Acknowledgments

We thank Nadine Henn and Iris Berg for technical assistance. This work was supported by grants from the Deutsche Forschungsgemeinschaft (Ho 2146/3-3, Schu 843/7-1, 7-2), Köln Fortune, and the Marga and Walter Boll-Stiftung (to U.C. Hoppe).

Received for publication August 24, 2009, and accepted in revised form January 20, 2010.

Address correspondence to: Uta C. Hoppe, University of Cologne, Department of Internal Medicine III, Kerpener-Str. 62, 50937 Cologne, Germany. Phone: 49.221.478.32396; Fax: 49.221.478.32397; E-mail: uta.hoppe@uni-koeln.de.

1. Murphy E. Primary and secondary signaling pathways in early preconditioning that converge on the mitochondria to produce cardioprotection. *Circ Res*. 2004;94(1):7–16.
2. Pong K. Ischaemic preconditioning: therapeutic implications for stroke? *Expert Opin Ther Targets*. 2004;8(2):125–139.
3. Heusch G, Boengler K, Schulz R. Cardioprotection: nitric oxide, protein kinases, and mitochondria. *Circulation*. 2008;118(19):1915–1919.
4. Goto M, Liu Y, Yang XM, Ardell JL, Cohen MV, Downey JM. Role of bradykinin in protection of ischemic preconditioning in rabbit hearts. *Circ Res*. 1995;77(3):611–621.
5. O'Rourke B. Mitochondrial ion channels. *Annu Rev Physiol*. 2007;69:19–49.
6. Costa AD, Garlid KD. Intramitochondrial signaling: interactions among mitoKATP, PKCepsilon, ROS, and MPT. *Am J Physiol Heart Circ Physiol*. 2008;295(2):H874–H882.
7. Dorn GW II, et al. Sustained in vivo cardiac protection by a rationally designed peptide that causes epsilon protein kinase C translocation. *Proc Natl Acad Sci U S A*. 1999;96(22):12798–12803.
8. Foster DB, Rucker JJ, Marban E. Is Kir6.1 a subunit of mitoK(ATP)? *Biochem Biophys Res Commun*. 2008;366(3):649–656.
9. Heinzel FR, et al. Impairment of diazoxide-induced formation of reactive oxygen species and loss of cardioprotection in connexin 43 deficient mice. *Circ Res*. 2005;97(6):583–586.
10. Boengler K, et al. Connexin 43 in cardiomyocyte mitochondria and its increase by ischemic preconditioning. *Cardiovasc Res*. 2005;67(2):234–244.
11. Li X, Heinzel FR, Boengler K, Schulz R, Heusch G. Role of connexin 43 in ischemic preconditioning does not involve intercellular communication through gap junctions. *J Mol Cell Cardiol*. 2004;36(1):161–163.
12. Boengler K, et al. Presence of connexin 43 in subsarcolemmal, but not in interfibrillar cardiomyocyte mitochondria. *Basic Res Cardiol*. 2009;104(2):141–147.
13. Er F, Michels G, Gassanov N, Rivero F, Hoppe UC. Testosterone induces cytoprotection by activating ATP-sensitive K+ channels in the cardiac mitochondrial inner membrane. *Circulation*. 2004;110(19):3100–3107.
14. Inoue I, Nagase H, Kishi K, Higuti T. ATP-sensitive K+ channel in the mitochondrial inner membrane. *Nature*. 1991;352(6332):244–247.
15. Zhou M, Diwu Z, Panchuk-Voloshina N, Haugland RP. A stable nonfluorescent derivative of resorufin for the fluorometric determination of trace hydrogen peroxide: applications in detecting the activity of phagocyte NADPH oxidase and other oxidases. *Anal Biochem*. 1997;253(2):162–168.
16. Forbes RA, Steenbergen C, Murphy E. Diazoxide-induced cardioprotection requires signaling through a redox-sensitive mechanism. *Circ Res*. 2001;88(8):802–809.
17. Cortassa S, Aon MA, Winslow RL, O'Rourke B. A mitochondrial oscillator dependent on reactive oxygen species. *Biophys J*. 2004;87(3):2060–2073.
18. Drose S, Hanley PJ, Brandt U. Ambivalent effects of diazoxide on mitochondrial ROS production at respiratory chain complexes I and III. *Biochim Biophys Acta*. 2009;1790(6):558–565.
19. Ye ZC, Wyeth MS, Baltan-Tekkok S, Ransom BR. Functional hemichannels in astrocytes: a novel mechanism of glutamate release. *J Neurosci*. 2003;23(9):3588–3596.
20. Chaytor AT, Evans WH, Griffith TM. Peptides homologous to extracellular loop motifs of connexin 43 reversibly abolish rhythmic contractile activity in rabbit arteries. *J Physiol*. 1997;503(Pt 1):99–110.
21. Eckardt D, et al. Functional role of connexin43 gap junction channels in adult mouse heart assessed by inducible gene deletion. *J Mol Cell Cardiol*. 2004;36(1):101–110.
22. Inagaki K, Begley R, Ikeno F, Mochly-Rosen D. Cardioprotection by epsilon-protein kinase C activation from ischemia: continuous delivery and antiarrhythmic effect of an epsilon-protein kinase C-activating peptide. *Circulation*. 2005;111(1):44–50.
23. Doble BW, Ping P, Kardami E. The epsilon subtype of protein kinase C is required for cardiomyocyte connexin-43 phosphorylation. *Circ Res*. 2000;86(3):293–301.
24. Baines CP, et al. Mitochondrial PKCepsilon and MAPK form signaling modules in the murine heart: enhanced mitochondrial PKCepsilon-MAPK interactions and differential MAPK activation in PKCepsilon-induced cardioprotection. *Circ Res*. 2002;90(4):390–397.
25. Palmer JW, Tandler B, Hoppel CL. Biochemical properties of subsarcolemmal and interfibrillar mitochondria isolated from rat cardiac muscle. *J Biol Chem*. 1977;252(23):8731–8739.
26. Jaburek M, Costa AD, Burton JR, Costa CL, Garlid KD. Mitochondrial PKC epsilon and mitochondrial ATP-sensitive K+ channel copurify and coreconstitute to form a functioning signaling module in proteoliposomes. *Circ Res*. 2006;99(8):878–883.
27. Ardehali H. Signaling mechanisms in ischemic preconditioning: interaction of PKCepsilon and MitoK(ATP) in the inner membrane of mitochondria. *Circ Res*. 2006;99(8):798–800.
28. Goodenough DA, Paul DL. Beyond the gap: functions of unpaired connexon channels. *Nat Rev Mol Cell Biol*. 2003;4(4):285–294.

29. Jiang JX, Gu S. Gap junction- and hemichannel-independent actions of connexins. *Biochim Biophys Acta*. 2005;1711(2):208–214.
30. Sugiura H, Toyama J, Tsuboi N, Kamiya K, Kodama I. ATP directly affects junctional conductance between paired ventricular myocytes isolated from guinea pig heart. *Circ Res*. 1990;66(4):1095–1102.
31. Saez JC, Retamal MA, Basilio D, Bukauskas FF, Bennett MV. Connexin-based gap junction hemichannels: gating mechanisms. *Biochim Biophys Acta*. 2005;1711(2):215–224.
32. Weiss JN, Korge P. The cytoplasm: no longer a well-mixed bag. *Circ Res*. 2001;89(2):108–110.
33. Mochly-Rosen D. Localization of protein kinases by anchoring proteins: a theme in signal transduction. *Science*. 1995;268(5208):247–251.
34. Riva A, Tandler B, Loffredo F, Vazquez E, Hoppel C. Structural differences in two biochemically defined populations of cardiac mitochondria. *Am J Physiol Heart Circ Physiol*. 2005;289(2):H868–H872.
35. Reaume AG, de Sousa PA, Kulkarni S, Langille BL, Zhu D, Davies TC, Juneja SC, Kidder GM, Rossant J. Cardiac malformation in neonatal mice lacking connexin43. *Science*. 1995;267(5205):1831–1834.
36. Rottlaender D, Matthes J, Vatner SF, Seifert R, Herzig S. Functional adenylyl cyclase inhibition in murine cardiomyocytes by 2'(3')-O-(N-methylanthraniloyl)-guanosine 5′-[gamma-thio]triphosphate. *J Pharmacol Exp Ther*. 2007;321(2):608–615.
37. Michels G, et al. Two distinct human voltage-gated Ca2+-channels regulate cardiac mitochondrial Ca2+-uptake. *Circulation*. 2009;119(18):2435–2443.
38. Xu W, et al. Cytoprotective role of Ca2+- activated K+ channels in the cardiac inner mitochondrial membrane. *Science*. 2002;298(5595):1029–1033.
39. Kirichok Y, Krapivinsky G, Clapham DE. The mitochondrial calcium uniporter is a highly selective ion channel. *Nature*. 2004;427(6972):360–364.
40. Siemen D, Loupatatzis C, Borecky J, Gulbins E, Lang F. Ca2+-activated K channel of the BK-type in the inner mitochondrial membrane of a human glioma cell line. *Biochem Biophys Res Commun*. 1999;257(2):549–554.
41. Gassanov N, Brandt MC, Michels G, Lindner M, Er F, Hoppe UC. Angiotensin II-induced changes of calcium sparks and ionic currents in human atrial myocytes: potential role for early remodeling in atrial fibrillation. *Cell Calcium*. 2006;39(2):175–186.
42. Lange PS, Er F, Gassanov N, Hoppe UC. Andersen mutations of KCNJ2 suppress the native inward rectifier current I(K1) in a dominant-negative fashion. *Cardiovasc Res*. 2003;59(2):321–327.
43. Michels G, et al. K+ channel regulator KCR1 suppresses heart rhythm by modulating the pacemaker current If. *PLoS ONE*. 2008;3(1):e1511.
44. Michels G, Er F, Khan IF, Südkamp M, Herzig S, Hoppe UC. Single-channel properties support a potential contribution of HCN channels and If to cardiac arrhythmias. *Circulation*. 2005;111(4):399–404.
45. Guo Y, Wu WJ, Qiu Y, Tang XL, Yang Z, Bolli R. Demonstration of an early and a late phase of ischemic preconditioning in mice. *Am J Physiol*. 1998;275(4 Pt 2):H1375–H1387.
46. Schwanke U, Konietzka I, Duschin A, Li X, Schulz R, Heusch G. No ischemic preconditioning in heterozygous connexin43-deficient mice. *Am J Physiol Heart Circ Physiol*. 2002;283(4):H1740–H1742.